Determination of water-cement ratios of hardened cement pastes based on the estimation of under-pixel porosity in backscattered electron images

著者	Hoang DangGiang, Igarashi Shinichi
雑誌名	International Journal of Structural Engineering
巻	4
号	1-2
ページ	4-13
発行年	2013-01-01
URL	http://hdl.handle.net/2297/33399

doi: 10.1504/IJSTRUCTE.2013.050760

Determination of water-cement ratios of hardened cement pastes based on the estimation of under-pixel porosity in backscattered electron images

Abstract

SEM-BSE image analysis technique is one of promising approaches to determine water/cement ratios in hardened cementitious materials. In this study, a method using under-pixel information in the BSE images is proposed. It is hypothesized that a gray level of each pixel reflects the under-pixel porosity. It is also assumed that the porosity smaller than the resolution results in the shifts in position of the gray levels of specific phases. The amounts of shifting are combined with the Powers and Brownyard model so that the degree of hydration is directly estimated from the BSE images. The method was applied to hardened cement pastes with different water/cement ratios. There was a good agreement between estimated and real water/cement ratios. An estimate within an error of ±0.02 was attained except an extremely low water/cement ratio. The shift in the gray level histogram is useful information on microstructure in cement pastes.

Keywords: w/c, backscattered electron image, gray level histogram, mean atomic number, image analysis, calcium hydroxide, CSH, unhydrated cement, capillary pores, under-pixel porosity, cement paste, cement gel, Powers and Brownyard model

1. Introduction

The mass ratio of water to cement is the key parameter to determine not only mechanical properties but also durability of concrete. These days, maintenance or performance evaluation for deteriorated concrete structures is a significant issue which must be rationally solved in terms of life cycle management. For the purpose of repairing or diagnosis of those deteriorated concrete structures, it is quite often required to know water/cement ratios of them. If an old concrete structure has been managed properly for a long time, we would not have any problem to know its water/cement ratio of record. However, in practice, it seems that management records cannot be always found for all the deteriorated concrete structures.

There have been proposed many methods to determine water/cement ratios of hardened concretes. In general, the method based on chemical analysis is used in Japan (CAJ, 1967). However, that method cannot be applied to concretes containing lime stone aggregate. Furthermore, skilled chemists are also necessary to obtain reliable results. The thin section method has been widely used in Scandinavian countries (Nordtest 1999). In this method, fluorescence microscopic examination is made for thin sections of concrete. It has been reported that this method gives an accurate estimate within an error of ± 0.02. However, the method needs many reference sections for comparison of brightness that represents porosity. The fluorescence microscopy method is criticised for not giving such a good accuracy in practice (Neville, 2003).

Imaging based on scanning electron microscope (SEM) examination may be a promising method to determine water/cement ratios of concrete. Sahu et al.(2004) have pointed out that there exists a linear relationship between porosities evaluated by the SEM-backscattered electron image (BSE) image analysis and water/cement ratios of hardened concretes. The present authors have also proposed a method that uses 3D particles size distribution of unhydrated cement particles identified in BSE images (Igarashi et al., 2005). In that method, cross sections of each unhydrated cement particle are converted to the 3D particle size using a procedure of spatial statistics. Recently, Wong and Buenfeld (2009) have also proposed a method that combines the SEM-BSE imaging and the traditional hydration model of Powers and Brownyard (1946). Their method is built on assumption that all the capillary pores are visible and properly segmented by a field emission scanning electron microscope (FE-SEM) examination. The FE-SEM has a better resolving power so that almost the entire range of capillary pores may be detected. However, as long as a conventional SEM with a tungsten filament is used, such a fine feature of microstructure is generally invisible. However, taking the principle of imaging in the BSE mode into account, microstructure smaller than a resolution must be at least reflected to a gray level for each individual pixel.

In this study, it is assumed that an observed gray level has information on microporosity, i.e. under-pixel porosity for a specific phase. It is also assumed in the whole gray level histogram that the locations of peaks for some phases are made to shift due to the under-pixel porosity. The amount of shifting in position is used for estimating the under-pixel porosity. Using the under-pixel porosity and other characteristic values directly obtained by the conventional SEM-BSE image analysis technique, a method to determine water/cement ratios of hardened cement pastes is proposed. Comparison between estimated and real values of water/cement ratio is discussed.

2. Experimental

2.1 Materials and mix proportions of cement pastes

The cement used was an ordinary Portland cement. Water/cement ratios of the cement pastes were 0.25, 0.40, 0.45, 0.50 and 0.60. A polycarboxylic acid type superplasticizer was used in cement pastes with a water/cement ratio of 0.25. Cylindrical specimens of 100 mm in length and 50 mm in diameter were produced in accordance with JIS R 5201. They were demolded at 24 hours after casting, and then cured in water at 20˚C until the prescribed ages.

2.2 BSE image analysis

At the age of 28 days, slices about 10mm in thickness were cut from the cylinders for the BSE image analysis. Their moisture was replaced progressively by ethanol and *t*-butyl alcohol. Then, they were frozen under the *t*-butyl alcohol, and dried under the vacuum. The dried specimens were impregnated with a low viscosity epoxy resin. After the resin hardened at room temperature, the slices were finely polished with SiC papers and diamond slurries.

Samples were examined using an SEM equipped with a quadrupole backscatter detector. The BSE images were acquired at a magnification of 500×. Taking account of statistical variations in the results of image analysis, ten fields in each specimen were randomly chosen and analysed. Each BSE image consists of 1148×1000 pixels. The size of one pixel is about 0.22×0.22μm. An overflow method was used to make binary segmentation based on the gray level histogram (Wong et al., 2006). Pixels for unhydrated cement particles, calcium hydroxide, CSH and pores were tallied to determine area fractions of those phases. Based on the stereology principle, the area fractions in 2D cross sections were regarded as 3D volume fractions of the phases of interest. An example of BSE image and its segmentation are given in Fig. 1.

3. How to determine water/cement ratios

3.1 Mean atomic numbers and brightness

Contrast of each phase in BSE imaging depends on its mean atomic number. Fig. 2 shows the relationship between backscattered electron coefficient η and atomic numbers. The coefficient is expressed as an increasing function with the atomic number. The mean atomic numbers of the constituent phases in cement paste are given in Table 1. They are not so large that the function is almost proportional to the atomic numbers in the range for the phases, as found in Fig. 1. This linear relationship suggests that there also exists a linear relationship between gray levels of each phase and their atomic numbers. Thus, if those phases identified in the SEM-BSE examination exhibit the gray levels that correspond to the pure compounds, the gray levels of the phases are uniquely determined by the atomic numbers. In other words, the nominal values of gray levels for the phases can be calculated theoretically.

3.2 Shifts of gray levels in position

Fig. 3 shows an example of gray level histogram obtained for a cement paste. The mean levels of each constituent phase (I_{Cement}, I_{CH}, I_{CSH}, I_{Pore}) are determined by a conventional image analysis procedure. For example, the gray level values of I_{Cement} and I_{Pore} are about 246 and 26, respectively. Using these values and the linear relationship between the gray levels in the range, as mentioned above, the theoretical values of gray levels for the intermediate phases of CH and CSH are calculated using Eq.[1] and [2].

$$I_{CHest} = I_{Pore} + \left(I_{Cement} - I_{Pore}\right)\frac{\overline{Z}_{CH} - \overline{Z}_{Pore}}{\overline{Z}_{Cement} - \overline{Z}_{Pore}} \quad [1]$$

$$I_{CSHest} = I_{Pore} + \left(I_{Cement} - I_{Pore}\right)\frac{\overline{Z}_{CSH} - \overline{Z}_{Pore}}{\overline{Z}_{Cement} - \overline{Z}_{Pore}} \quad [2]$$

Where, $\overline{Z}_{Pore}$, $\overline{Z}_{CSH}$, $\overline{Z}_{CH}$ and $\overline{Z}_{Cement}$ are the mass-weighted mean atomic numbers for pores, CSH, CH and unhdrated cement, respectively. The gray levels calculated for CH and CSH phases are about 213 and 193, respectively. However, these calculated values are clearly different from the values actually obtained by the image analysis. In particular, the position of the level for CSH phase is greatly changed.

3.3 Reason for the shifts of gray levels

Comparing the gray levels between theoretically estimated and actually analysed values, the latter has shifted toward the lower level of gray scale. In other words, the gray levels actually obtained were always smaller than the calculated ones. This fact suggests that those phases contain phases of which gray levels are lower than the nominal value for them. Fig. 4 shows BSE images of a cement paste with a water/cement ratio of 0.60. Unhydrated cement particles of the brightest phase and capillary pores of the darkest one are clearly visible. In addition to those distinct phases, light gray regions of CH with irregular shapes are seen, as squared in Fig. 4(a). If the CH region is examined at a greater magnification, the phase is found inhomogeneous. It also contains black particles that are finer pores, as found in Fig. 4(b). This suggests that the shifts of the gray levels toward the darker direction result from the presence of fine capillary pores that are not detected at the magnification.

3.4 Evaluation of under-pixel porosity for CH and CSH

CSH phase identified by the image analysis is actually a heterogeneous phase such that other hydration products such as CAH coexist in the phase. As found in Table 1, the range of the weighted mean atomic number for CSH is wider than those of other phases. Therefore, it is difficult to determine a specific shift in gray scale. Contrary to the CSH phase, CH is a crystalline phase so that the mean atomic number is uniquely determined. Therefore, once the gray level of CH phase in an image is obtained following the image analysis procedure, it is easy to calculate a specific shift in gray level between the observed and the calculated values.

However, it should be noted that there are two phases that shift the gray level of CH phase toward lower values. One is porosity smaller than the resolution. The other is CSH that has a lower gray level than that for CH. However, taking account of differences in mechanism of precipitation for those two phases, it is assumed that CH does not intermingle with CSH in a phase observed at the magnification. Then, the shift in the gray level for CH can be attributed only to the coexistence of microporosity, i.e. under-pixel porosity. As the gray level for pores is known, the under-pixel porosity δ in CH phase is calculated by Eq.[3].

$$\delta = \frac{I_{CHest} - I_{CH}}{I_{CHest} - I_{Pore}} \approx \frac{I_{CHest} - I_{CH}}{I_{CHest}} \qquad [3]$$

As for the CSH phase, it also contains the under-pixel porosity. This results in the shift in gray level of the CSH. The under-pixel porosity in CSH can be different from that in CH since one is amorphous while the other is crystalline. Their precipitation mechanisms are different from each other. However, as mentioned previously, it is difficult to determine a specific shift in gray level for the CSH phase. Furthermore, taking account of the fact that CSH and CH phases are treated together as a cement gel in the hydration model of Powers and Brownyard (1946), it is also assumed here that the CSH phase has the same under-pixel porosity as the CH phase.

3.4 How to determine the initial volume fractions of cement and water

Following the method described above, the under-pixel porosity is determined. Apart from the estimation of the under-pixel porosity, coarse capillary porosity is easily determined by the conventional image analysis procedure. The total capillary porosity is the sum of them. If the total capillary porosity and the volume fraction of unhydrated cement are subtracted from the total volume, i.e. the whole area of observation window for the SEM-BSE examination, a volume fraction of solid hydration product including gel pores is estimated. In other words, the amount of cement gel produced during the hydration of cement is determined. If the hydration model of Powers and Brownyard (1946) is used, hydration of cement of 1cc produces 2.1cc of hydration products. Using this relation, it is easy to determine the amount of cement that is consumed for producing the cement gel calculated above. Thus, the initial cement content is obtained as the sum of the unhydrated cement and the consumed cement. If a complementary space of the initial volume of cement is considered as a space occupied with mixing water, the volume fraction of water is determined. If the density of cement is properly assumed, then the initial water/cement ratio is estimated. The whole procedure to determine water/cement ratios of cement pastes is given in Fig. 5 as a flow diagram.

4. Results and discussion

Fig.6 shows comparison of water/cement ratios between estimated and real values. The proposed method overestimated 6% of the ratio for the cement paste with a water/cement ratio of 0.25. The estimated values for other cement pastes are almost comparable to the real ones. The differences in water/cement ratios between them are at most 2%. If an estimate within ±0.05 is allowable by the rule of

thumb that is generally accepted, the proposed method can be used as a reliable way for estimating water/cement ratios of hardened cement pastes. It should be noted that the method sufficiently covers a range of water/cement ratios of old concrete structures for which estimation of water/cement are often requested for a diagnosis purpose.

Comparison of the total capillary porosity between different estimation methods is given in Table 2. The total capillary porosity that was directly identified by the FE-SEM image analysis (Wong and Buenfeld, 2009) was almost the same as the value evaluated by the proposed method. This suggests that the evaluation of under-pixel porosity from the shift in the gray level histogram was correct. Furthermore, the capillary porosity evaluated by this method was also the same as the value that was obtained by a conventional image analysis method (Igarashi et al., 2004). In the conventional method, the degree of hydration of cement is calculated using the volume fraction of residual cement obtained from BSE images and the initial cement content that is known a priori. Of course, different ordinary Portland cements were used in those cement pastes. Therefore, it is not appropriate to find agreements among the values. However, such an agreement between different methods suggests that the degree of hydration of cement is estimated with a sufficient accuracy if the volume fraction of hydration products is correctly measured from BSE images. Following the procedure proposed in the method, it is not necessary to know the initial cement content. Only the information obtained from BSE images is enough for estimating water/cement ratios. This would be greatly advantageous when an old concrete structure missing official records is required to evaluate its mix proportion.

On the other hand, the method proposed in this study is applied only to cement paste specimens that are cured in water continuously for 28 days. Taking account of practical situations in determining water/cement ratios, the method must be extended to mature concretes that contain aggregate particles and little unhydrated cement. Furthermore, they may deteriorate under various circumstances. It is very difficult to segment an aggregate phase based on its gray levels from BSE images. Presence of cracks and few particles identified as cement and CH phases also make image operations difficult. The present authors have also proposed a method to make a segmentation of aggregate particles from images of low magnification, which sufficiently cover a representative volume element for the distribution of aggregate particles (Hoang and Igarashi, 2009). Multiscale imaging to cover from micro porosity to large particles of aggregate may be

necessary to establish a reliable method for determining water/cement ratios of concretes. Further study is needed for applying the proposed method to concrete.

5. Conclusions

A method to determine water/cement ratios of hardened cement pastes was proposed. The method is based on simple image operations for BSE images. Major results obtained in this study are as follows;

(1) Actual gray levels of CH and CSH phases identified in BSE images were different than the levels estimated from the mean atomic numbers. The difference in gray level was defined as the shift due to the presence of under-pixel pores.

(2) The shift for CH phase was used for evaluating the under-pixel porosity of the entire cement gel.

(3) The volume fraction of solid hydration product containing gel pores was evaluated by subtracting the coarse capillary porosity, the unhydrated cement and the under-pixel porosity from the total volume of cement paste.

(4) The amount of cement consumed during hydration was calculated using the Powers and Brownyard model. The initial cement content was obtained as the sum of the consumed cement and the unhydrated cement that is directly evaluated from BSE images.

(5) There exists a good agreement between estimated water/cement ratios and real ones. They were within an error of ± 0.02, except for an extremely low water/cement ratio.

(6) The total capillary porosity estimated by the proposed method was comparable to the porosity that was evaluated by the conventional image analysis technique.

Acknowledgements

A part of this study was supported by the Japan Society for the Promotion of Science, Grant-in-Aid for Scientific Research (C), #21560482, 2009-2011.

References

CAJ (1967) ‘Report on the method to determine mix proportions of hardened concrete’, F-18, Cement Association Japan, (in Japanese).

Dang, G.H., Igarashi, S. and Naito, D. (2009) ‘Segmentation of aggregate and estimation of particle size distribution from images of concretes’, Proceedings of the Japan Concrete Institute, Vol.31, No.1, pp.2065-2070 (in Japanese).

Igarashi, S., Kawamura, M. and Watanabe, A. (2004) ‘Analysis of cement pastes and mortars by a combination of backscatter-based SEM image analysis and calculations based on the Powers model’, Cement and Concrete Composites, Vol.26, No.8, pp.977-985.

Igarashi, S., Ikezaki, Y. and Watanabe, A. (2005) ‘Determination of degree of hydration and water/cement ratio by three dimensional particle size distribution of unhydrated cement in concrete’, Concrete Research and Technology, Vol.16, No.1, pp.87-95 (in Japanese).

Neville, A.M. (2003) ‘How closely can we determine the water-cement ratio of hardened concrete?’ , Materials and Structures, Vol.36, No.259, pp. 311-318.

Nordtest (1999) ‘Concrete, hardened: water-cement ratio’, Nord Test, NT Build 361.

Powers, T.C. and Brownyard, T.L. (1946-47) ‘Studies of the physical properties of hardened cement pastes (Nine parts)’, Journal of American Concrete Institute, No.43.

Sahu, S., Badger, S., Thaulow, N. and Lee, R.J. (2004) ‘Determination of water-cement ratio of hardened concrete by scanning electron microscopy’, Cement and Concrete Composites, Vol.26, No.8, pp.987-992.

Wong, H.S., Head, M.K. and Buenfeld, N.R. (2006) ‘Pore segmentation of cement-based materials from backscattered electron images’, Cement and Concrete Research, Vol.36, No. 6, pp.1083-1090.

Wong, H.S. and Buenfeld, N.R. (2009) ‘Determining the water-cement ratio, cement content, water content and degree of hydration of hardened cement paste: Method development and validation on paste samples’, Cement and Concrete Research, Vol.39, No.10, pp.957-965.

Table 1 Mean atomic numbers $\overline{Z}$ weighted by relative atomic mass

Compounds	Notation	$\overline{Z}$
Alite	C_3S	15.1
Belite	C_2S	14.6
Aluminate	C_3A	14.3
Ferrite	C_4AF	16.7
Calcium hydroxide	CH	14.3
Calcium silicate hydrate	C-S-H	≈11.7~14.2

Table 2 Comparison of the total capillary porosites obtained by different image-based methods (W/C=0.40, Age=28d)

Wong & Buenfeld (2009)	This study	Igarashi et al.(2004)
19.3	19.1	17.8

unit :vol%

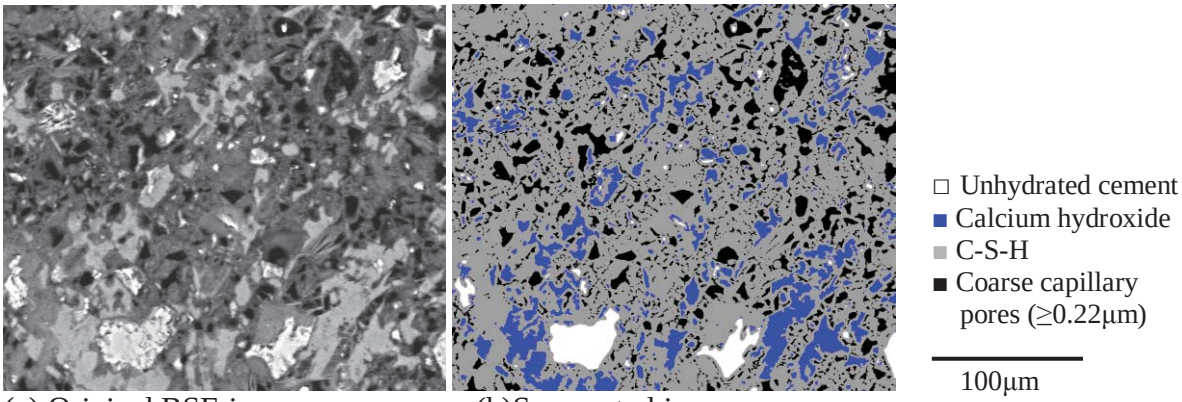

(a) Original BSE image (b)Segmented image

Fig. 1 BSE image and its segmentation into four different phases

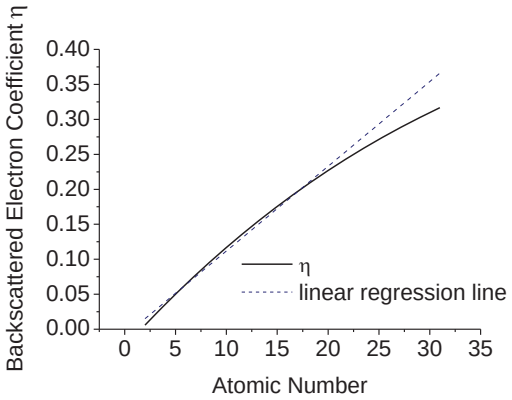

Fig. 2 Backscattered electron coefficient η vs. atomic number

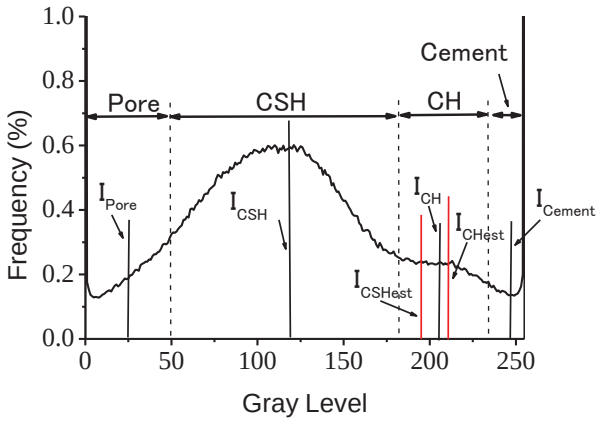

Fig. 3 Schematic diagram to explain the shifts of gray levels for CSH and CH phases

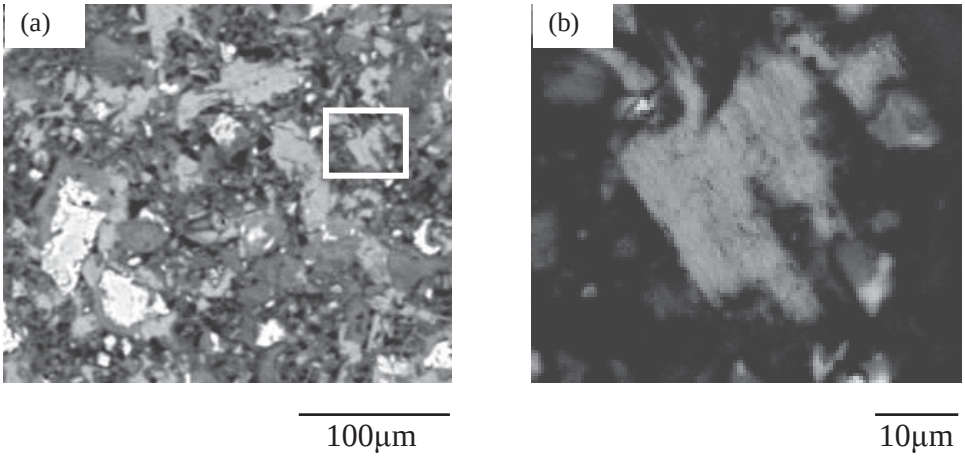

Fig. 4 Presence of under-pixel pores in a CH paricle (a)BSE image (b)Enlargement of the squared area for CH phase in (a)

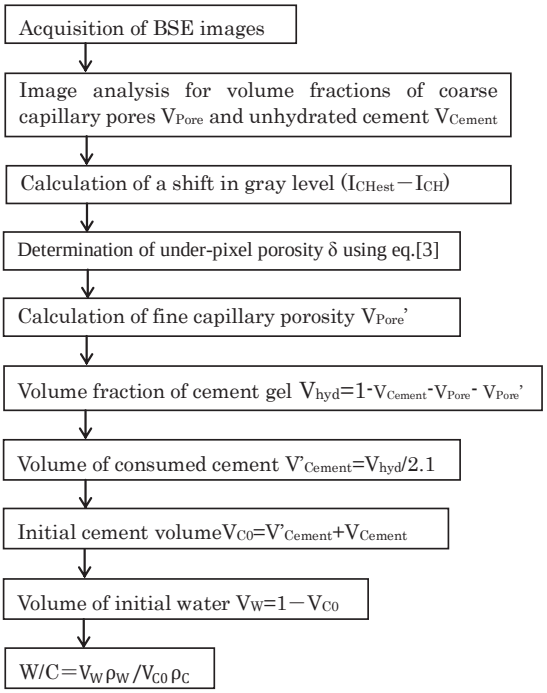

Fig. 5 Flow of the procedure to determine water/cement ratios of hardened cement pastes

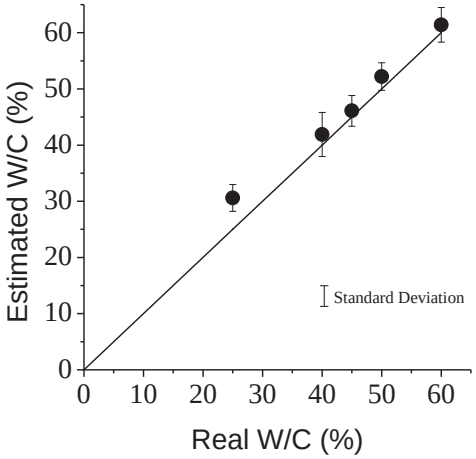

Fig. 6 Comparison of water/cement ratios between estimated and real values